Energy Conversion and Management 81 (2014) 534–546

Contents lists available at ScienceDirect

Energy Conversion and Management

journal homepage: www.elsevier.com/locate/enconman

Numerical and experimental study of combustion, performance and emission characteristics of a heavy-duty DI diesel engine running on diesel, biodiesel and their blends

Luka Lešnik *, Jurij Iljaž, Aleš Hribernik, Breda Kegl

University of Maribor, Faculty of Mechanical Engineering, Smetanova 17, SI-2000 Maribor, Slovenia

ARTICLE INFO

Article history:
Received 23 December 2013
Accepted 17 February 2014

Keywords:
Heavy-duty diesel engine
Biodiesel
Mixing controlled combustion model
Sub-model for parameter determination
Emissions

ABSTRACT

The presented paper introduces a performed study into the possibility of replacing mineral diesel fuel with pure biodiesel fuel or their blends with diesel fuel. The presented work was carried out experimentally and numerically on a heavy-duty bus diesel engine using mineral diesel fuel, neat biodiesel fuel made from rapeseed oil and their 25% (B25), 50% (B50) and 75% (B75) blends. The influence of biodiesel fuel and blends on engine combustion, performance and emission characteristics was studied experimentally on an engine test-bed and numerically using an AVL BOOST simulation program. A new empirical sub-model for determining a combustion model parameters was proposed within a BOOST program. All the model's parameters were determined regarding the properties of the tested fuel and engine speed. The obtained results show a reduction in engine power and torque when increasing the percentage of biodiesel fuel in the fuel blends due to lower calorific value of biodiesel fuel. Higher oxygen content in the biodiesel and blends contributed to a better oxidation process within the combustion chamber, which resulted in a reduction of carbon oxides (CO) and nitrogen oxides (NO_x) at three different engine speeds (1360, 1700 and 2000 min^{-1}) and full throttle position. Both the experimental and numerical results indicated that neat biodiesel or biodiesel-diesel blends can be used within a heavy-duty diesel engine with modified static fuel delivery angle (injection pump timing) of the mechanically-controlled injection system.

1. Introduction

Methyl esters of vegetable oils known as biodiesel are attracting increasing interest because of their low environmental impact and their potential as an alternative fuel. The consumption of biodiesel is increasing from year to year. It is stimulated by the raising of crude oil prices, the striving of individual countries to reduce their dependence on imported energy sources, and implementing the Kyoto protocol directives for the reduction of global emissions from greenhouse gasses [1]. World biodiesel production increased by more than 20 times in 2012 compared to 1990. At the same time ethanol production has increased more than 7-fold which makes biofuels fuels more accessible and attractive for commercial usage [2–4]. Many EU countries are already mixing biofuels with conventional fuels to meet European Union demand for biofuel usage in transportation.

Usage of biofuels mixtures with conventional fuels or usage of pure biofuels requires experimental and numerical testing of their influences on engine operating conditions and emission formation. Experimental testing is usually very costly and time-consuming and therefore numerical simulations are commonly used when performing parametric studies of biofuels' influences on engines' operating conditions, combustion process and emission formations. Detailed analyses of fuel spray-jet development within a combustion chamber and analyses of emission formation zones are usually made using complex 3D simulations [5]. Parametric studies of biofuels' influences on engine performance and emission formation are usually made using thermodynamic or phenomenological combustion models because they are significantly less time-consuming than 3D simulations and enable us to simulate the whole engine operation under several engine operating conditions, which make it possible to numerically perform engine emissions' test-cycles, etc. In phenomenological and thermodynamic combustion models the complex dynamics of air-flow, spray development and emission formation are replaced by model parameters. Model parameters hold some crucial information about spray

* Corresponding author.
E-mail address: llesnik@gmail.com (L. Lešnik).

http://dx.doi.org/10.1016/j.enconman.2014.02.039
0196-8904/

Nomenclature

Q	heat (J)
I	integral
α	angle (°CA)
τ	duration (°CA/ms)
C	constant/parameter
k	density of turbulent kinetic energy
E	energy (J)
λ	air excess ratio
CV	calorific value (MJ/kg)
CN	cetan number
X	oxygen content

Subscripts

c	cylinder
PMC	premixed combustion
$IDCF$	ignition delay calibration factor
UB	unburned zone
ref	reference
id	ignition delay
SOI	start of injection
fv	vaporized fuel
kin	kinetic
f,inj	fuel injected
$diff$	diffusion
$stoich$	stoichiometric
f	fuel
$turb$	turbulence
$diss$	dissipation
epx	experimentally obtained
ns	numerically obtained

Abbreviation

D2	diesel fuel
B100	pure biodiesel fuel
B25	mixture of 25% biodiesel fuel with D2
B50	mixture of 50% biodiesel fuel with D2
B75	mixture of 75% biodiesel fuel with D2
CO	carbon monoxide
CO_2	carbon dioxide
O_2	oxygen
NO_x	nitrogen oxides
HC	hydro carbon
MCC	mixing controlled combustion
NLPQL	non-linear programming by quadratic Lagrangian
CA	crank angle
BTDC	before top dead center
L–M	Levenberg–Marquardt
BSFC	break specific fuel consumption

development, combustion speed, and injection delay and therefore their accurate determination is necessary. Different engines and different fuels require different parameters values. The values for some parameters for commonly used combustion models and engines are already known but when a new type of fuel is introduced their determination needs to be based on user experience. Therefore, the results from experimental measurements are needed to confirm the results of numerical simulations and for properly selecting the values for combustion model parameters.

Combustion process in internal combustion engine highly depends on the start of injection process and its strategy. The injection timing influence on duration of fuel ignition delay phase which has further influence on premixed combustion phase, engine performance and emission formation process. Park et al. [6] studied the influence of different injection timing on engine performance and emission formation when running on diesel–ethanol and diesel–ethanol–biodiesel fuel mixtures. The effect of different injection strategies within a heavy-duty diesel engine on engine performance and emission formation were studied by Thumheer et al. [7]. Possibility to replace conventional fuels with biofuels with aim to reduce harmful emission formation has been studied in many papers. Studies can be made under full engine load (full throttle position) and different engines speeds or under different engine loads and different engine speeds. Roy et al. [8] tested how biodiesel fuels from pure and used canola oil influenced a direct injection diesel engine's performance and emission formation at high idling operations. Silitonga et al. [9] tested how properties of *Ceiba pentandra* biodiesel blends influence on performance and exhaust emissions of a diesel engine on different engine speeds at full engine load (full throttle position). The influence of rape seed oil biodiesel on engine combustion and emission formation at different engine loads and speeds was studied by Qi et al. [10], in work of Kegl and Hribernik [11–13] and in work done by Yamane et al. [14]. Holwan and Joshi [15] tested how different ethanol, diesel and biodiesel fuel mixtures' influence on engine performance and emission formation on several different engine loads. Some studies were also made using less known biofuels like fish oil fuel [16], KDV synthetic diesel fuel [17] and biogas [18] in compression ignition engines. Emission formation in diesel engines can also be reduced by adding additives in diesel or biodiesel fuels. Palash et al. [19] tested the impact of NO_x reducing antioxidant additive on performance and emissions of a multi-cylinder diesel engine fueled with Jatropha biodiesel blends.

It is generally known that the usage of biodiesel fuel reduces engine power and torque due to their lower calorific values. In engines with mechanically-controlled injection systems this leads to increased break-specific fuel consumption. Replacing mineral diesel fuel with biodiesel fuels can contribute to reduction of exhaust gas emissions, which highly depend on engine load and engine speed. Holwan and Joshi [15], Silitonga et al. [9] and Qi et al. [10] obtained reduction of NO_x emissions on full engine load when increasing the percentages diesel fuel while Labeckas and Slavinskas [17] obtained increase of specific NO_x emissions production when using synthetic diesel fuel. Yamane et al. [14] obtained decrease of produced NO_x emissions when running on different biodiesel fuels at full engine load. When increasing percentage of biofuel the reduction of CO emissions was obtained in [15,14,10]. Higher CO emissions were obtained when using *Ceiba pentandra* biodiesel blends on full engine load (full throttle position) [9], when using synthetic diesel fuel [17] and by usage of 70% mineral diesel fuel mixed with 30% rapeseed oil biodiesel fuel in commercial truck diesel engine [20].

Some of the investigations have been made using both experimental testing and numerical simulations. Experimental results are necessary for verifying those numerical results which depend on proper selection of combustion model parameters. Combustion model parameters need to be determined for all tested fuels on each engine's operating regime. This process is time-consuming and requires the results of experimental measurements for its validations. The dependency of numerical results from proper parameter selection needs to be minimized if only numerical simulations are to be used for performing parametric studies of biofuel's influence on engine performance and emission formation. The results of experimental measurements can also be used for

determining model parameters. The capability of a non-linear programming by quadratic Lagrangian (NLPQL) optimization algorithm employed for tuning parameters of the Vibe combustion model was analyzed in work of Prah and Katrašnik [21]. They tested the influences of different objective (merit) functions and constrains on the accuracy of the results. Their work presented an innovative approach on how the parameters of Vibe combustion model can be determined based on the results of experimental measurements.

This presented paper concerns an experimental and numerical study regarding the influences of neat biodiesel fuel, mineral diesel fuel and their blends on the combustion, performance and emission characteristics of a heavy-duty diesel engine with a mechanically-controlled injection system. All testing was carried out on optimal static fuel delivery angles, determined in the previous paper [22]. The optimal injection pump timing for mineral diesel fuel D2 fuel was 23 °CA before the top dead center (BTDC), 22 °CA BTDC for B25, 21 °CA BTDC for B50, 20 °CA BTDC for B75, and 19 °CA BTDC for pure biodiesel fuel B100. Experimental measurements were obtained on an engine test-bed using MAN D2566 MUM four stroke heavy-duty diesel engine. Engine torque, power, in-cylinder pressure, brake-specific fuel consumption, HC, soot, O_2, NO_x and CO emissions were acquired during all measurements. Experimental testings' were repeated numerically with use of AVL BOOST simulation program and their mixing controlled (MCC) combustion model. A new sub-model for determining combustion model parameters based on the used fuels' properties and engine speeds is proposed in the presented paper. First, the determination of combustion model parameters for D2 and B100 fuels was presented as an inverse problem, which was solved using the Levenberg–Marquardt (L–M) optimization method. Experimentally measured in-cylinder pressure trace was used as a fitting parameter for the optimization method's objective function. The determined values of model parameters were further used for deriving a new empirical sub-model for the calculation of combustion model parameters. The proposed sub-model, which presents a novelty within the field of engine simulations, was then used for calculating the needed combustion model parameters for all five tested fuels. Finally, the influences of neat biodiesel fuels and their blends with mineral diesel fuel on engine power, torque, in-cylinder pressure, rate of heat release (ROHR), brake-specific fuel consumption (BSFC), NO_x and CO emissions were tested numerically and experimentally, followed by comparisons between the numerical and experimental results.

2. Tested fuels

Neat biodiesel fuel B100 produced from rapeseed oil at Biogoriva, Rače, Slovenia, and mineral diesel fuel D2 that contained no additives, were used during the presented study. Three mixtures of D2 and B100 were made at ratios of 25% (B25), 50% (B50) and 75% (B75) of biodiesel mixed with diesel fuel. The tested fuels' properties are presented in Table 1 and in Fig. 1.

Table 1
Tested fuels properties.

Fuel	D2	B25	B50	B75	B100
Density at 15 °C (kg/m^3)	838.8	850.3	861.8	873.3	884.8
Kinematic viscosity at 30 °C (mm^2/s)	3.34	3.8825	4.425	4.9675	5.51
Surface tension at 30 °C (N/m)	0.0255	0.026125	0.02675	0.027375	0.028
Caloric value (MJ/kg)	42.8	41.65	40.5	39.35	38.2
Cetan number	45	46.5	48	49.5	51
Stoichiometric air–fuel ratio	14.7	14.275	13.85	13.425	13
Flash point (°C)	66	84.125	102.25	120.375	138.5
Fuel composition					
Mass fraction C	0.86	0.83875	0.8175	0.79625	0.775
Mass fraction H	0.134	0.13075	0.1275	0.12425	0.121
Mass fraction S	0.003	0.0025	0.002	0.0015	0.001
Mass fraction O	–	0.025975	0.05195	0.077925	0.103
Ester content (%(m/m))	–	24.325	48.65	72.975	97.3
Total glycerol (%(m/m))	–	0.044	0.088	0.132	0.176
Monoglycerides content (%(m/m))	–	0.1475	0.295	0.4425	0.59
Diglycerides content (%(m/m))	–	0.035	0.07	0.105	0.14
Triglycerides content (%(m/m))	–	0.0125	0.025	0.0375	0.05
Water content (mg/kg)	50	75	100	125	150
Sulfur content, WD-XRF (mg/kg)	31	24.7	18.4	12.1	5.8

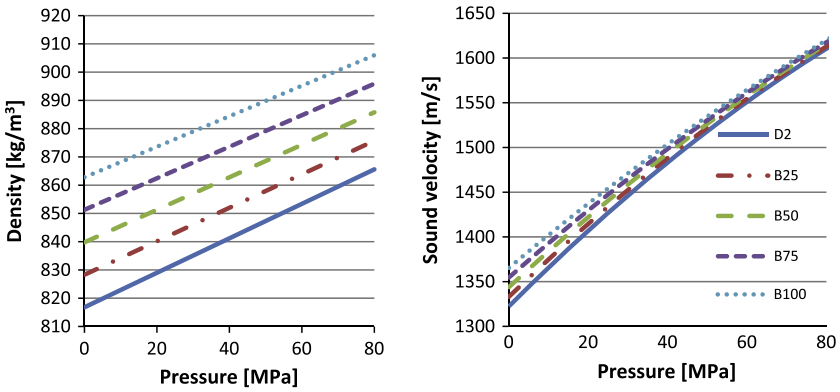

Fig. 1. Tested fuels' densities and sound velocities.

Some of the fuels' properties presented in Table 1 were measured using different test methods which corresponded to European or other standards. The fuels' densities were measured at 15 °C according to the European standard EN ISO 12185, kinematic viscosities were measured at 40 °C using a test method confirming the European standard EN ISO 3104, and the fuels' compositions were measured using the test method ASTM D 5291. Other presented fuel properties were supplied by producers of diesel and biodiesel fuels and were not further tested. In order to consider the actual properties of the tested fuels in numerical simulations, the properties from Table 1 were implemented within the BOOST program. Values of tested fuels' densities and sound velocities presented in Fig. 1 were calculated using equations derived in Ref. [23].

3. Experimental set-up

The experimental measurements were performed on a 6 cylinder naturally aspirated, water cooled MAN D2566 MUM four stroke heavy-duty diesel engine with M-combustion system. Some of the engine's characteristics are presented in Table 2. The experimental set up, presented in Fig. 2, consists of heavy-duty diesel engine, engine break (dynamometer), fuel and air consumption meters, in-cylinder pressure transducer and emissions analyzers. Engine was equipped with Bosch high pressure in-line injection pump with 6 plungers and 6 high pressure fuel lines. Engine tests were made on 1360, 1700 and 2000 engine speed under full throttle position. Under full throttle position maximal quantity of each tested fuel was delivery in engine which obtained maximal load for each fuel on all engine speeds. Different fuel properties, especially lower calorific value of biodiesel fuel and its blends, influence on maximal archived engine load for each fuel which can be seen in results. Static fuel delivery angle was set on optimal value for each fuel based on emission results of ESC 13 Mode test cycle, determined in previous study [22]. Optimal values of static fuel delivery angles are presented in Table 2.

Table 2
Engine specification.

Engine type	MAN D2566 MUM four stroke
Gas exchange	Natural aspirated
Number of cylinders	6
Bore (mm)	125
Stroke (mm)	155
Total displacement (ccm)	11,413
Compression ratio	17.5
Fuelling	Direct injection
Fuel pump	BOSCH PES6A95D410LS2542
Nozzle	BOSCH DLLA 5S834
Static fuel delivery angle (° BTDC)	23-D2; 22-B25; 21-B50; 20-B75; 19-B100

Measurements were split in five sections, in each section one test fuel was used and optimal static fuel delivery angle for used fuel was set. First all experimental measurements were made using pure diesel fuel to determine baseline engine operating characteristics and baseline emissions values. After measurements with diesel fuel were done, fuel lines were cleaned and static fuel delivery angle was set on 22°BTDC for B25 fuel. Experimental measurements were repeater for B25 fuel mixture. The whole measurement procedure was repeated for B50 and B75 fuel mixtures and for pure biodiesel fuel.

Results of measured engine power, torque and in-cylinder pressure were monitored and stored with data acquisition system for what a computer application was built in LabVIEW software. Engine power and torque were measured using Zöllner B – 305

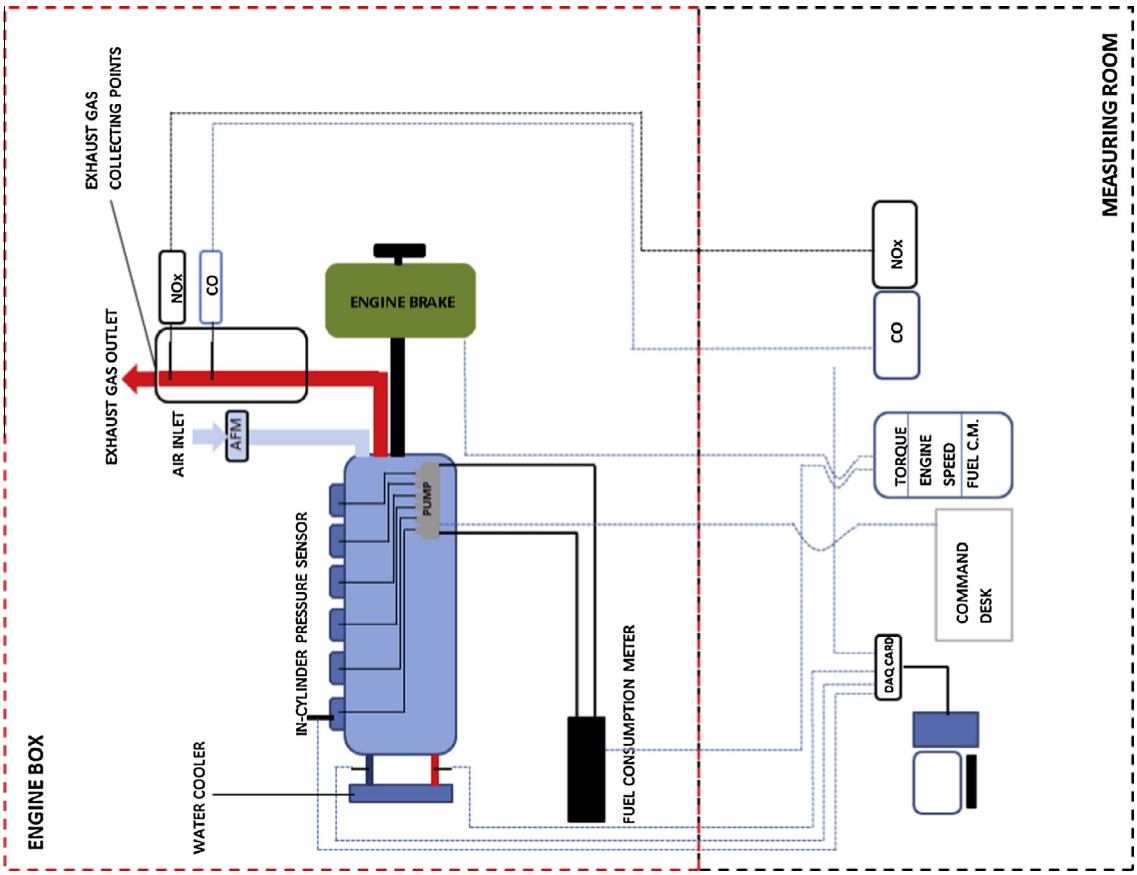

Fig. 2. Engine test bed scheme.

AC eddy current engine brake (dynamometer). Engine brake is designed to operate in range of 0–6500 rotation per minute and measure engine torque up to 2000 N m with accuracy ±0.2% of measuring range (MR). Kistler 6001 piezoelectric pressure transducer with measuring range 0–250 bar and accuracy ±0.8% of MR was mounted in combustion chamber of first engine cylinder for measuring in-cylinder pressure trace. The measurement of in-cylinder pressure started approximately 20 °CA BTDC and ended approximately 60 °CA after top dead center. Start of in-cylinder pressure measurement was triggered by the position of top dead center indicator mounted on engine flywheel. The values of measured in-cylinder pressure were stored by the computer application at intervals of 0.1 °CA rotation. For measuring engine air consumption RMG Messtechnik GmbH air flow meter was used. The air flow meter was placed on the engine intake port. Engine fuel consumption was measured using AVL Fuel Balance 730 dynamic measuring system. The fuel measuring system calculates hourly fuel consumption based on the difference of fuel mass in measuring vessel in specific time interval. AVL Fuel Balance 730 allows measurements of fuel consumption up to 150 kg/h with accuracy ±0.12% of MR.

Samples of exhaust gases were collected from the exhaust gas pipe for the analyses of NO_x and CO emissions content. A chemiluminescence analyzer from Thermoenvironmental Instruments Inc. was used for measuring the concentration on NO_x emissions in exhaust gases. The analyzer measure the amount on NO_x molecules in exhaust gases based on the amount of detected light emissions which are byproduct of chemiluminescent reaction of $NO + O_3$ in $NO_2 + O_2$. Measuring range of NO_x analyzer is from 0 ppm to 10,000 ppm with the accuracy ±1% of MR. The concentration of CO emissions in exhaust gasses was measured using non-dispersive infrared MAIHAK UNOR 610 analyzer. The analyzer measures the concentration of CO emissions in exhaust gasses based on absorption of an emitted infrared light through exhaust gas sample. The accuracy of CO analyzer was ±1% of measuring range from 0 to 1000 ppm.

Several OMEGA type J thermocouples were placed at different positions for measuring air, oil and exhaust gas temperatures. Measuring range of thermocouples was −40 to 750 °C with accuracy of ±1.5 °C.

The accuracy of measuring (equipment) results is presented in Table 3.

The rate of heat release curves were predicted from measured in-cylinder pressure traces with the use of a one-zone zero dimensional combustion model. The used combustion model is described in detail in [24].

4. Simulation model

The simulation model was created using the AVL BOOST simulation program. The used program was developed for the numerical analyses of engine cycles, gas exchanges and exhaust gasses after treatment. A Chmela and Orthaber MCC combustion model [25] was used for calculating the diesel engine's performance. NO_x emissions' formation was calculated using a Pattas and Häfner emission model [26], while CO emissions were calculated using an Onorati CO formation model [27]. Used MCC combustion model was elaborated by the AVL experts and is a property of AVL Company [28]. The most important equations of MCC combustion model are presented in next section. For detailed description of combustion model refer to Refs. [28,29].

Table 3
The accuracy of measured engine performance and emissions.

Measurements	Range of equipment	Accuracy of equipment
Engine torque	0–2000 N m	±0.2% of full range
In-cylinder pressure	0–250 bar	±0.8% of full range
Fuel consumption	0–150 kg/h	±0.12% of full range
NO_x emissions	0–10,000 ppm	±1% of full range
CO emissions	0–1000 ppm	±1% of full range
Temperature	−40 to 750 °C	±1.5 °C

4.1. Combustion model

The heat released during the fuel combustion within the combustion chamber is the only source of energy within internal combustion engines. The MCC combustion model divides combustion into two stages. The first stage is premixed or kinetic combustion which occurs after the ignition delay interval ends. The second part of the combustion is the mixing controlled or diffusion combustion that follows the premixed part of the combustion and begins when all the fuel/air mixture from the first part of the combustion has burned. The total released heat Q_c may be written as a sum of the heat released during premixed combustion Q_{PMC} and the heat released during mixing controlled combustion Q_{MCC}:

$$Q_c = Q_{PMC} + Q_{MCC} \tag{1}$$

In the premixed part of combustion the fuel which was vaporized and mixed with fresh air during the ignition delay interval is burned, therefore the fuel/air mixture burns rapidly. The Vibe function was used to predict the rate of heat released during the premixed part of combustion. The shape parameter in Vibe function was set at 2 for this purpose and the Vibe parameter at 6.9. The premixed combustion model parameter in Vibe function needs to be set by user and defines the amount of combusted fuel mass, injected during the ignition delay. Detailed description of Vibe function can be found in [28,29].

The duration of ignition delay τ_{id} and the crankshaft angle α_{id} at which the ignition delay ends (start of the combustion), were calculated using the ignition delay model, Eq. (2), developed by Andree and Pachernegg [25,28].

$$\frac{dI_{id}}{d\alpha} = \frac{1}{C_{IDCF}} \cdot \frac{T_{UB} - T_{ref}}{Q_{ref}} \tag{2}$$

where the individual notations in the equations represent:

I_{id} – ignition delay integral,
C_{IDCF} – ignition delay calibration factor,
T_{UB} – unburned zone temperature,
T_{ref} – reference temperature and
Q_{ref} – reference activation energy.

The reference temperature was set at 505 K. The reference activation energy was determined from the program's database based on fuel calorific value and oxygen content. When the ignition delay integral reached the value $\geqslant 1$, the ignition delay was calculated using the following equation [28]:

$$\tau_{id} = \alpha_{id} - \alpha_{SOI} \tag{3}$$

where α_{SOI} represents the start of the injection. Start of injection was defined with injection rate curve, which must be defined as an input data in BOOST program, and was calculated for each fuel on all operating regimes using BKIN mathematical program [30]. Start of combustion is calculated by BOOST program.

During the mixing controlled part of the combustion the fuel which was injected after the start of combustion is burned. The model assumed that the total amount of released heat during this stage of combustion Q_{MCC} was a function of the fuel available for combustion and the turbulent kinetic energy density within the cylinder [28]. The rate of heat released during this part of combustion is written as:

$$\frac{dQ_{MCC}}{d\alpha} = C_{comb} \cdot \left(m_{fv} - \frac{Q_{MCC}}{LCV} \right) \cdot w_{O2,a} \cdot C_{Rate} \cdot \frac{\sqrt{k}}{\sqrt[3]{V_c}} \quad (4)$$

where the individual notations in the equations represent:
C_{comb} – combustion constant,
m_{fv} – vaporized fuel mass,
$w_{O2,a}$ – oxygen available for combustion,
C_{Rate} – mixing rate constant,
k – local density of turbulent kinetic energy and
V_c – cylinder volume.

Combustion constant C_{comb} influences the fuel combustion speed. Higher values result in higher combustion speeds. It has a great influence on the shape of the rate of heat release curve.

The local density of the turbulent kinetic energy k is a function of the mixing rate constant C_{Rate} and the cylinder volume V_c and can be calculated by using the following equations [28]:

$$k = \frac{E_{kin}}{m_{f,inj} \cdot (1 + \lambda_{diff} \cdot m_{stoich})} \quad (5)$$

$$\frac{dE_{kin}}{dt} = 0.5 \cdot C_{turb} \cdot \dot{m}_f (v_{inj})^2 - C_{diss} \cdot E_{kin}^{1.5} \quad (6)$$

where the individual notations in the equations represent:
E_{kin} – kinetic jet energy,
$m_{f,inj}$ – injected fuel mass,
λ_{diff} – air excess ratio for diffusion burning,
m_{stoich} – stoichiometric mass of fresh charge,
C_{turb} – turbulent energy production constant,
$\dot{m}_f$ – fuel mass flow,
ρ_f – fuel density,
v_{inj} – fuel injection velocity and
C_{diss} – dissipation constant.

Turbulent energy production constant and dissipation constant control the influence of fuel spray jet kinetic energy and dissipation on the combustion process.

4.2. Emission formation models

The emission model used for the computation of NO_x formation in the presented study, is based on the Pattas and Häfner NO_x formation model [26,28]. The CO emission formation model used is based on the Onorati CO formation model [27,28]. For detailed description of emissions models used in presented study please refer to Ref. [28,29].

5. New empirical sub-model

The combustion model's parameters are usually determined based on user experience. Their influence on the combustion process can be predicted from those equations presented in the previous chapter. Several simulations test runs are usually needed for accurate determination of the combustion model's parameters. Proper selection of combustion model parameters is validated by a comparison between the experimentally and numerically obtained results, which can be very time-consuming. If the results of the experimental measurements are known or can be obtained, they can be used for determining the combustion model's parameters.

This paper therefore proposes a new empirical sub-model for the determination of combustion model parameters. The proposed sub-model will allow the calculating of values for each combustion model parameter based on tested fuel properties and engine speed. Engine load will not be included in the equation while it cannot be determine in advance without experimental measurements. Determination of combustion models' parameters for diesel and bio-diesel fuels was first presented as an inverse problem which was solved using the Levenberg–Marquardt (L–M) optimization method, where the combustion model's parameters presented design variables during the optimization process. The Levenberg–Marquardt optimization method (L–M) is a very popular curve-fitting method. The experimentally measured in-cylinder pressure trace was used as a fitting parameter within the objective function for optimization.

The objective function for optimization was defined for minimizing the difference between the simulation results and the experimentally obtained results of in-cylinder pressure trace. The formulation of objective function F for optimization process is presented in the following equation:

$$F(x) = \frac{1}{2} \sum_{i=1}^{n} (p_{exp,i} - p_{ns,i})^2; \quad i = 1, \ldots, 30 \quad (7)$$

Only three combustion model parameters were defined as design variables during the optimization process. The selected parameters were the ignition delay calibration factor C_{IDCF}, combustion constant C_{comb} and the premixed combustion model parameter C_{PMC}. The ignition delay in the compression ignition engines was predicted by the integration of Eq. (6), thus even if the ignition delay were known from the experimental results, C_{IDCF} could not be calculated. The C_{PMC} parameter depends on the duration of the ignition delay period and therefore cannot be determined in advance either. The combustion constant has great influence on the shape of in-cylinder pressure trace, ROHR, engine power, and torque. Its value can be estimated from known fuel properties but cannot be precisely determined, therefore C_{comb} was also defined as a design variable during the optimization process. It was because of the nature of the M-combustion system, where more than 90% of fuel is injected onto the wall of the combustion chamber that the dissipation constant C_{diss} was set at constant for all the tested fuels. The amount of kinetic energy which enters the combustion chamber with the fuel jet is controlled by the turbulence energy constant C_{turb}. The value of the turbulence constant depends on the actual mass of injected fuel $m_{f,inj}$ and the injection velocity v_{inj} (Eqs. (5) and (6)). The actual injected fuel mass and time needed for injection were determined from the experimental results obtained regarding the engine injection systems for each operating regime, as presented in a previous study [29]. Average injection velocities for each fuel were calculated from the experimental results and the values of the models' parameters were set based on the ratios of average injection velocities for all the fuels tested. All the values of combustion model parameters were set within the prescribed limit intervals from 0 to 2, suggested by the developers of the BOOST program.

The forms of the equations for determining each parameter were selected from the values of combustion models' parameters obtained during the optimization process. It was for that purpose that the program for testing the accuracies of different forms of equations was made in Mathematica, where the accuracies of several forms of equation were tested using the coefficient of determination R^2. Those equations' calculated values for parameters D2 and B100 were compared to the values for the parameters determined during optimization. The R^2 values for the selected equations were greater than 0.99, thus providing good accuracy for the selected equation of the proposed sub-model. The selected equations are just one of the possible forms of equations which do not represent the only possible forms of the equations. The influence of engine speed n and fuel calorific value CV of the values of C_{IDCF} can be seen in Fig. 3. Similar trends can be obtained for other parameters.

The following forms of equation were selected as equations for the new sub-model regarding combustion model parameter determination:

$$C_{IDCFi,j} = -0.057931 \cdot e^{n_j} \cdot CN_i + 0.377201 \cdot n_j \cdot CN_i + 6.56338 \cdot n_j^2 - 25.6968 \cdot n_j - 0.326347 \cdot CN_i + 25.1403 \quad (8)$$

$$C_{combi,j} = -0.286503 \cdot e^{n_j} \cdot CV_i + 1.35589 \cdot n_j \cdot CV_i + 74.8476 \cdot n_j^2 - 227.799 \cdot n_j - 0.722727 \cdot CV_i + X_i + 171.666 \quad (9)$$

$$C_{PMCi,j} = -0.025944 \cdot n_j \cdot CN_i + 0.0638479 \cdot n_j^2 + 0.933666 \cdot n_j + 0.0335885 \cdot CN_i - 1.10891 \quad (10)$$

where n_j represents engine speed divided by 1000 at specific engine operating regime j, CV_i calorific value, CN_i cetan number of fuel i and X_i fuel oxygen content.

Ignition delay calibration factor C_{IDCF} was expressed as a function of fuel cetan number CN_i and engine speed n_j. Fuel cetan number defines the ability of fuel to ignite in compression ignition engines and is a significant indicator of the fuel quality. Fuels with a better ability for ignition have higher cetan numbers and vice versa. Therefore CN_i has a great impact on the ignition delay period, C_{IDCF} parameter, and also on the amount of fuel mass that will burn in the premixed part of the combustion, as defined by C_{PMC}. The combustion constant C_{comb} defines the fuel combustion speed during the diffusion part of the combustion process. Combustion speed is limited by the speed of fuel vapor formation and by the diffusion of air (oxygen) molecules in combustion front. Combustion speed also influences the shape of the rate regarding the heat release curve, which is influenced by the fuel's calorific value. Both, fuel oxygen content X_i and calorific value CV_i, are included in equations for calculating the combustion parameter.

Good agreement between values for those parameters determined during the optimization process (opti.) and with the proposed sub-model's calculated values (sub-model) can also be seen in Table 4. Some differences (dif.) between the determined and calculated values of C_{IDCF} are noticable at lower engine speeds for both fuels. The calculated values of C_{comb} are the same as the optimization process determined values. The differences between the calculated and determined values of C_{PMC} parameters are rather small.

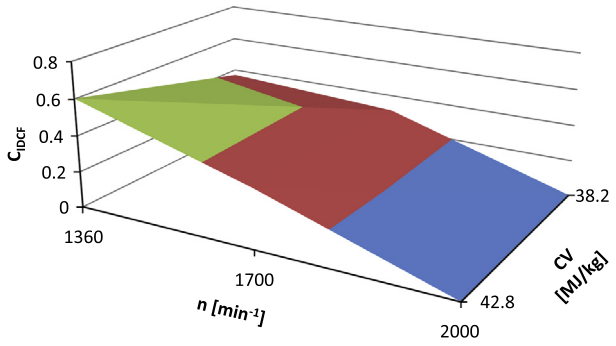

Fig. 3. Influence of engine speed and fuel calorific value on C_{IDCF}.

6. Results

The influences of pure biodiesel fuel and their blends with mineral diesel fuel on heavy-duty diesel engine performance, in-cylinder pressure, rate of heat release (ROHR), brake-specific fuel consumption (BSFC) and emission formation were tested experimentally and numerically. All testing was performed at full throttle position (full engine load) and three different engine speeds, 1360 rpm, 1700 rpm and 2000 rpm. The tests were made on optimal static fuel delivery angle for each fuel tested. The static fuel delivery angle of biodiesel fuel started 4° of crank angle later than the static fuel delivery of pure diesel fuel. Despite the fact that pure biodiesel's influence on advanced injection start in mechanically-controlled injection systems, the static fuel delivery angle shift will influence on the later start of biodiesel injection compared with the diesel fuel. This will lead to a later start of combustion which will have an influence on later pressure, temperature and rate of heat release rises when using B100. Optimal static fuel delivery angles for all fuels are presented in Table 2.

The combustion model parameters for numerical simulations were calculated using new proposed empirical sub-model.

Figs. 4–6 present the experimentally and numerically obtained results of engine torque, power, break specific fuel consumption (BSFC) and emissions.

Increasing percentages of biodiesel in the fuel mixture caused a reduction of fuel calorific value, Table 1, increase fuel density and kinematic viscosity. The differences in calorific value of biodiesel fuel will influence on reduction of engine power when running on pure biodiesel fuel and its mixtures with diesel fuel. Higher fuel density of mixtures and pure biodiesel fuel influence on greater mass of injected fuel in mechanical controlled injection systems which compensate the reduction of biodiesel fuel calorific value. In some engine operating regimes greater amount of injected fuel mass of biodiesel fuel or its mixture can cause increase of engine power compared to pure diesel fuel.

The experimental and numerical results presented in Figs. 4–6 show good agreement between the numerically and experimentally results of engine rated torque, power and break specific fuel consumption. The reduction of engine power and torque, compared to diesel fuel, was obtained experimentally on lower engine speed for mixtures and for pure biodiesel fuel. Numerically obtained results also indicate on reduction of engine power and torque on lower engine speed for B100 and all fuel mixture, except for B75 which show an increase of obtained engine power and torque Fig. 4. The increase of engine power and torque was also obtained experimentally and numerically on 1700 and 2000 engine rotation speeds when running on B25 fuel mixture. When using pure

Table 4
Comparison of determined and calculated values of combustion model parameters.

	C_{IDCF}			C_{comb}			C_{PMC}		
D2									
n (min^{-1})	1360	1700	2000	1360	1700	2000	1360	1700	2000
Opti.	0.603	0.324	0.0001	0.512	1.316	9.983	0.202	0.191	0.189
Sub-model	0.574	0.324	0.0001	0.512	1.316	9.983	0.203	0.189	0.190
Dif. (%)	5.052	0	0	0	0	0	0.493	1.058	0.526
B100									
n (min^{-1})	1360	1700	2000	1360	1700	2000	1360	1700	2000
Opti.	0.368	0.311	0.0001	0.588	1.351	10.674	0.193	0.125	0.081
Sub-model	0.339	0.311	0.0001	0.588	1.351	10.674	0.193	0.126	0.080
Dif. (%)	8.554	0	0	0	0	0	0	0.794	1.250

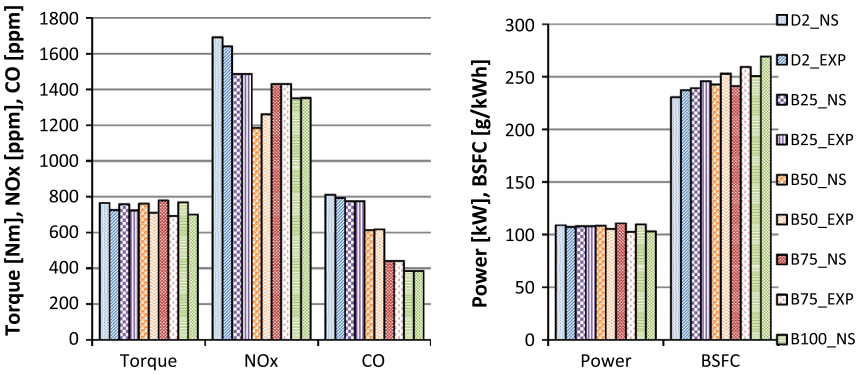

Fig. 4. Experimental and numerical results at 1360 rpm.

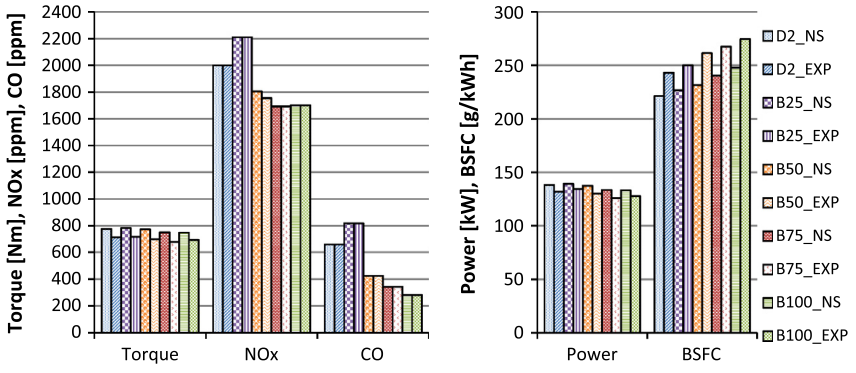

Fig. 5. Experimental and numerical results at 1700 rpm.

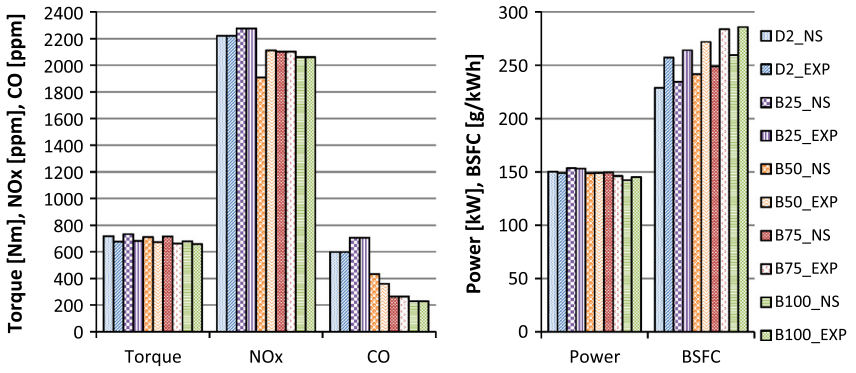

Fig. 6. Experimental and numerical results at 2000 rpm.

biodiesel fuel, B50 and B75 fuel mixture experimentally and numerically obtained results of engine power and torque on 1700 and 2000 min^{-1} are lower than when running on pure diesel fuel. The maximal decrease the engine's rated power was within the range of 5–10% and can be observed at all operating regimes when comparing the results for pure biodiesel with those for diesel fuel. The maximal decrease the engine's rated torque was also within the range of 5–10% for B100 and D2 fuels. The experimentally-determined engine power and torque are 5–10% lower than the numerically obtained results of engine power and torque.

Biodiesel fuel properties influence on advance injection start when using pure biodiesel fuel or its mixtures in mechanical controlled injection system [29]. Advance injection timing and higher density of biodiesel fuel influence on greater amount of injected biodiesel fuel per one engine cycle, which further influence on higher hourly fuel consumption [29]. Greater amount of injected biodiesel fuel mass per engine cycle and lower engine rated power increased engine break specific fuel consumption when running on pure biodiesel fuel and its blends. The increase of specific fuel consumption when running on biodiesel fuel was obtained experimentally and numerically on all engine speeds. The 10–12% highest BSFC was observed when using pure biodiesel fuel compared to pure mineral diesel fuel. Lower experimentally obtained engine rated power influence on higher experimental break specifics fuel consumption BSFC on all engine operating regimes, Figs. 4–6. In general numerical and experimental results indicate on same trend of BSFC increase when increasing the percentage of biodiesel fuel in fuel mixture.

Differences in chemical composition properties of diesel and biodiesel fuel influence on different mass fraction of C, H, S and O components in biodiesel fuel mixtures. Fuel properties, optimal static fuel delivery angle for each fuel and different engine speeds

influence on amount of produced emissions on full throttle position. Maximal amount of produced NO_x and CO emissions on low engine speed was obtained both experimentally and numerically when using pure diesel fuel. The lowest concentration of nitrogen oxides on low engine speed was obtained experimentally and numerically when running on B50 fuel mixture Fig. 4. Increasing engine speed increased production of NO_x emissions. The highest amount of produced NO_x emission on 1700 and 2000 min^{-1} was obtained experimentally and numerically with usage of B25 fuel mixture. The lowest NO_x emissions on 1700 engine speed were obtained experimentally and numerically when using B75 fuel mixture. Numerical results on 2000 min^{-1} that the lowest NO_x emissions were obtained with B50 fuel mixture while experimental results show the lowest NO_x emissions when using B100 fuel. Experimental and numerical results of CO emissions indicates that when running engine on full throttle position the lowest CO was obtained when using pure biodiesel fuel on all engine speeds. In general increasing the percentage of biodiesel fuel in fuel mixture decreases the production of CO emissions on all engine speeds. Some disagreements with previous argument are seen when using B25 fuel mixture on 1700 and 2000 min^{-1}, which caused increase of experimentally and numerically obtained results of CO emissions.

Figs. 7 and 8 are presenting the results of experimental and numerical specific emissions.

Increasing engine speed causes an increase in production of specific NO_x emissions and reduction of specific CO emissions. The lowest specific NO_x emissions were obtained experimentally and numerically when using B50 fuel mixture on all engine speeds. Only numerical results on 1700 min^{-1} indicate that the lowest specific NO_x emissions were obtained when using B75 fuel mixture. Slighter increase of specific CO emissions is observed both experimentally and numerically when using B25 fuel mixture on 1700 rpm. The values of experimental results of specific emissions are slightly higher than numerical results because of lower experimental engine rated power.

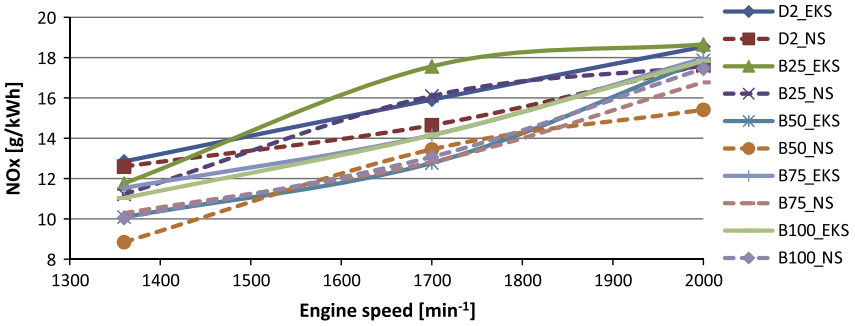

Fig. 7. Experimental and numerical results of specific NO_x emissions.

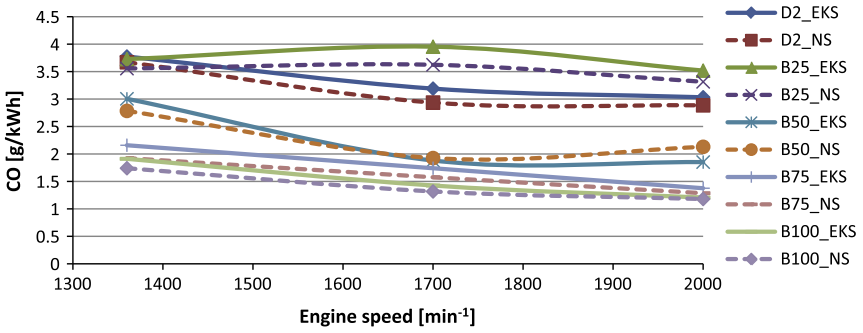

Fig. 8. Experimental and numerical results of specific CO emissions.

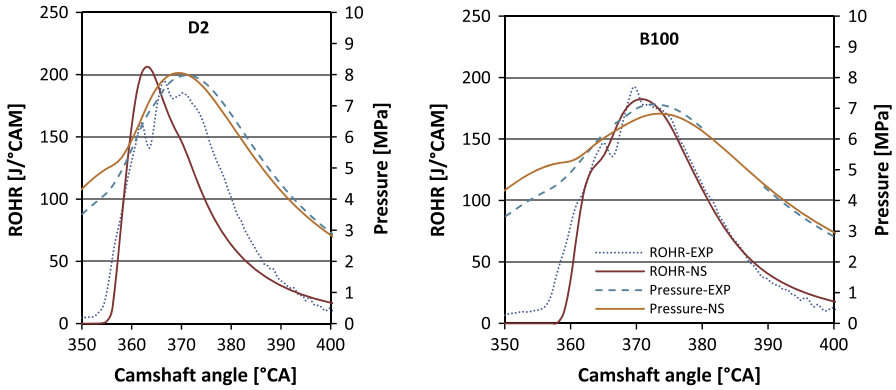

Fig. 9. Rate of heat release and in-cylinder pressure for D2 and B100 fuels at 1360 rpm.

The results for the numerically-obtained and measured in-cylinder pressure for D2 and B100 fuels are presented in Figs. 9–11. These figures also present the experimentally and numerically obtained curves of rate of heat release (ROHR).

The numerical and experimental results of in-cylinder pressure indicate that when using pure biodiesel fuel in heavy-duty diesel engine with M-combustion system maximal value of pressure decrease on all engine speeds. The maximal pressure is achieved both numerical and experimental at 2000 rpm using D2 where the maximal engine power was obtained, which is reasonable. All experimental and numerical differences in maximal in-cylinder pressure reduction when using pure biodiesel fuel were within the range of 5–10%, only on 2000 rpm approximately 15% reduction in maximal value of in-cylinder presser was obtained. The reduction of in-cylinder pressure when running on pure biodiesel fuel influence on small reduction of maximal values of rate of heat release curves. Maximal decrease of ROHR curve values was obtained with numerical results on 2000 rpm when running on pure biodiesel fuel. The reduction of in-cylinder pressure and ROHR is caused by both later injection of biodiesel fuel (retarded static fuel delivery angle) and decrease of biodiesel calorific value.

Figs. 12–14 are presenting the results of numerical and experimental obtained in-cylinder pressure and rate of heat release for B25, B50 and B75 fuel mixtures.

The experimental results of measured in-cylinder pressure on all engine speeds indicate that when increasing percentage of biodiesel fuel in fuel mixture maximal values of in-cylinder pressure are reduced. Same trend was also obtained numerically on maximal engine speed Fig. 12. On lower engine speed increase of maximal in-cylinder pressure was obtained numerically when

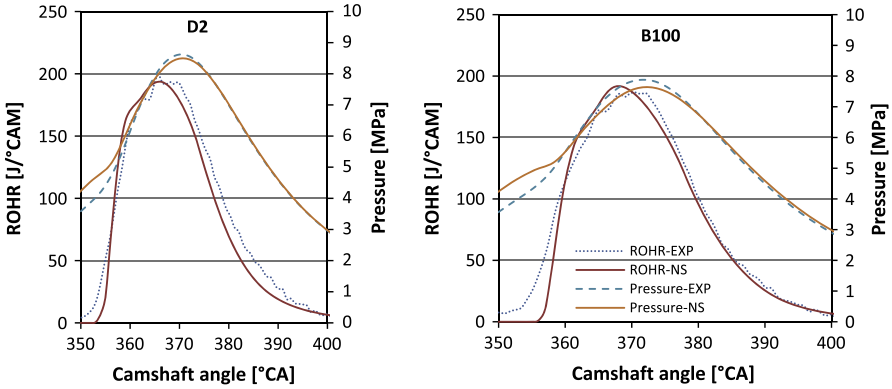

Fig. 10. Rate of heat release and in-cylinder pressure for D2 and B100 fuels at 1700 rpm.

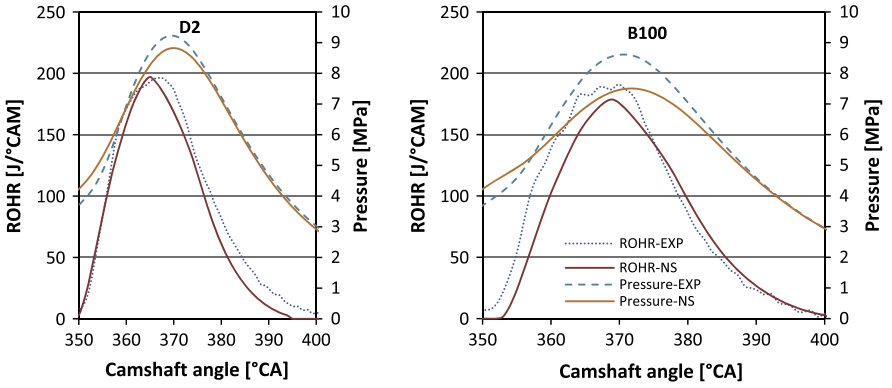

Fig. 11. Rate of heat release and in-cylinder pressure for D2 and B100 fuels at 2000 rp.

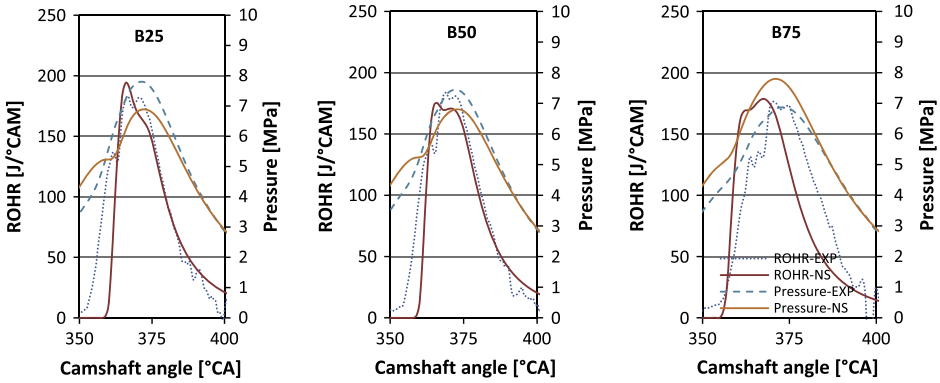

Fig. 12. Rate of heat release and in-cylinder pressure for B25, B50 and B75 fuels at 1360 rpm.

using B75 fuel compared to B25 fuel. The increase of maximal value of in-cylinder pressure, compared to B25 fuel mixture, was also obtained numerically when using B50 fuel mixture at 1700 engine rpm. Variances in numerical obtained results of maximal in-cylinder pressure, compared to experimental results, are probably caused due to improper determination of combustion model parameters determined with new proposed sub-model.

All presented ROHR curves have a form, typical for engines with M-combustion systems, which does not have distinctive kinetic combustion phase.

Fig. 15 present numerical results of ignition delay. From the presented results can be seen that increasing percentage of biodiesel fuel decreases ignition delay period on low engine speed. Decrease of ignition delay when increasing percentage of biodiesel fuel was also obtained at 1700 and 2000 engine rpm but is significant lower than it's the reduction on low engine speed. On decrease of ignition delay integral influence higher biodiesel fuel cetan number and retarded static fuel delivery angle which caused later injection of biodiesel fuel. The in-cylinder pressure and temperature are higher with every ° of CA closer to top dead center which influence on better atomization of biodiesel fuel which also contributes to decrease of ignition delay interval.

The computed in-cylinder temperature and emission formations for D2 and B100 fuels are presented in Figs. 16–18.

It can be seen from Figs. 16–18 that the combustion of pure biodiesel fuel at the optimal static fuel delivery angle reduces maximal value of in-cylinder temperature. The most evident reduction can be seen on maximal engine rated power, Fig. 18. From all results of in-cylinder temperature can be seen that when using B100 fuel the start of temperature rise is delayed because of the later start of fuel injection (retarded static fuel delivery angle). Both NO_x and CO emission formation rates reduced because of the later

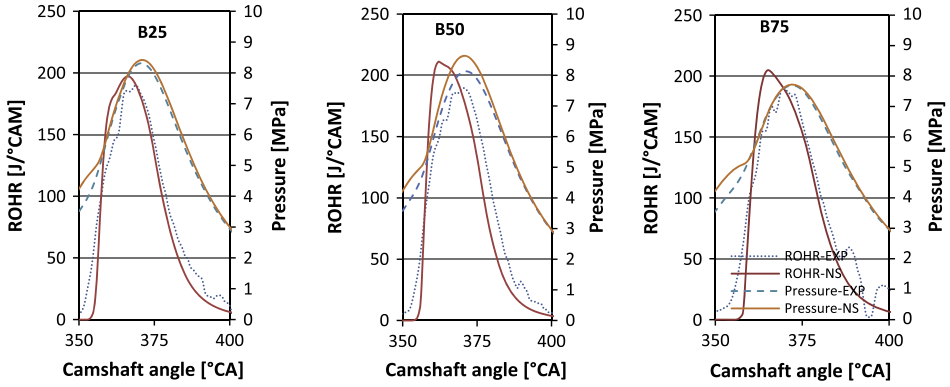

Fig. 13. Rate of heat release and in-cylinder pressure for B25, B50 and B75 fuels at 1700 rpm.

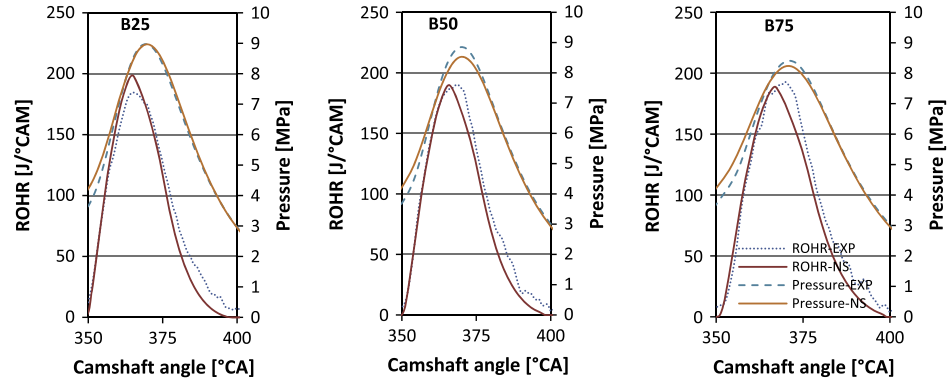

Fig. 14. Rate of heat release and in-cylinder pressure for B25, B50 and B75 fuels at 2000 rpm.

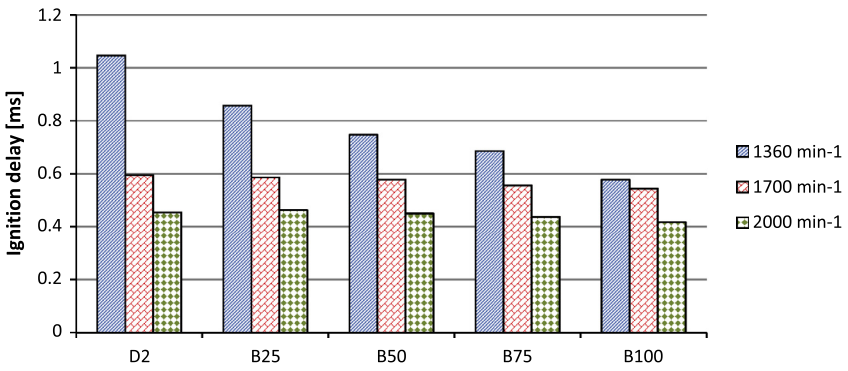

Fig. 15. Numerical results of ignition delay.

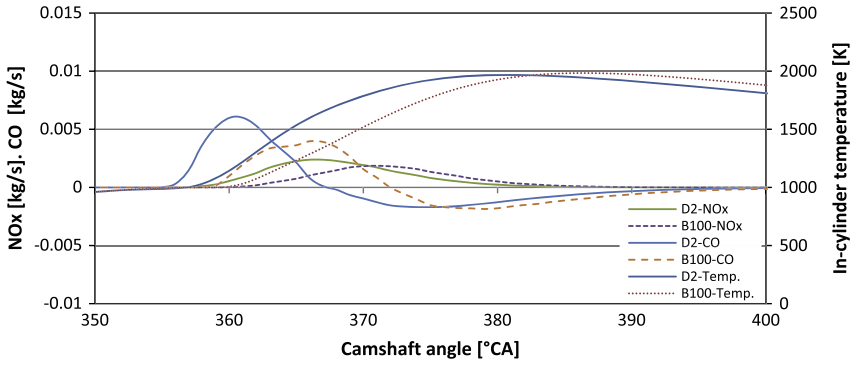

Fig. 16. In-cylinder temperature and emission formation at 1360 rpm.

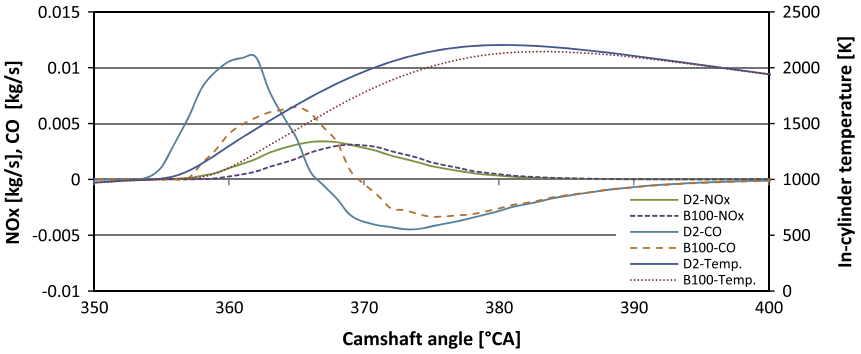

Fig. 17. In-cylinder temperature and emission formation at 1700 rpm.

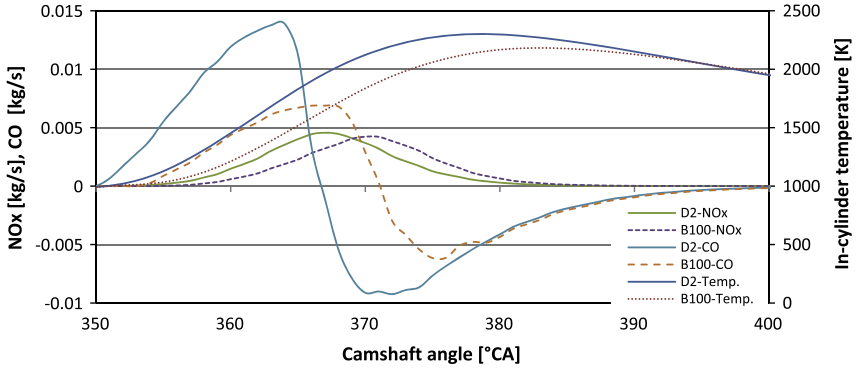

Fig. 18. In-cylinder temperature and emission formation at 2000 rpm.

rises of in-cylinder pressure and temperature. Lower maximal in-cylinder temperature also slowed down the emission formations. The higher content of oxygen in pure biodiesel fuel contributed to a better oxidation process in the combustion chamber and reduced the CO emissions formation rate, while lower in-cylinder temperature reduced thermal NO_x formation rate on full engine throttle position. Negative values of CO formation rates are obtained on all engine speeds after approximately 360 °CA. The reduction of CO emissions formation rate is the result of CO molecules reaction with O_2 to produce CO_2 emissions.

7. Conclusions

The influence of neat biodiesel fuel, mineral diesel fuel and their blends on the combustion, performance and emission characteristics of a heavy-duty diesel engine was studied numerically and experimentally. All measurements and simulations were made on optimal static fuel delivery angle (optimal injection pump timing) for each fuel tested. Experimental measurements were performed on an engine test-bed equipped using several different measuring systems and an engine dynamometer. Numerical simulations were made using the AVL BOOST simulation program and a mixing controlled combustion model. A new empirical sub-model for determining combustion model parameters was implemented into the mixing controlled combustion model. All the measurements and numerical simulations were made under full throttle position (full engine load) and various engine speeds (1360, 1700 and 2000 rpm). Based on the obtained results, the following conclusions can be made:

- Increasing percentage of biodiesel fuel in fuel mixtures decreases the fuel's calorific value, which further reduces the rated engine power and torque. Maximal differences were observed when comparing the results for D2 and B100 fuels. It was within the range of 5–10% for engine rated power and engine rated torque. Numerical results of engine rated power

and torque are approximately 10% higher than experimental results. The presented results of engine rated power and torque show reasonable agreement between the numerical and experimental results.

- The decreased fuel calorific value increases engine brake-specific fuel consumption in both experimental and numerical results. When using pure biodiesel fuel BSFC is 12% higher than when using pure mineral diesel fuel. BSFCs for fuel mixtures are between values of D2 and B100 fuels. Lower values of experimentally determined power and torque increased experimental results of BSFC compared to numerical results.
- When using pure biodiesel fuel, lower in-cylinder temperature, pressure and rate of heat release were observed. Experimental results of in-cylinder pressure and ROHR also indicate a reduction of maximal values of pressure and rate of heat release rate when using biodiesel fuel mixtures. The results of numerical simulations are not so fully consistent to experimental results. Pressure increase was obtained when using B75 fuel on 1360 rpm and by usage of B50 fuel on 1700 rpm. Other results follow the trend of experimental measurements.
- Lower in-cylinder temperature reduces thermal NO_x emissions formation. The oxygen contents within the biodiesel fuel and blends contributed to a better oxidation process within the combustion chamber which caused a reduction in CO emission formations.
- NO_x and CO emission reductions were observed when increasing the percentage of biodiesel fuel in the fuel mixture at all engine speeds. Slighter increases of NO_x and CO emissions were observed only for B25 fuel at 1700 and 2000 rpm. The lowest CO and the highest NO_x emissions were observed at maximal engine power. Production of NO_x and CO emissions highly depend on engine operating regime therefore the presented results can only apply to full throttle position (full engine load for each tested fuel) and optimal static fuel delivery angles, which both influence on amount of produced emissions.
- The newly proposed empirical sub-model used for determining the combustion model's parameters presents a useful tool for determining combustion model parameters based on tested fuel properties and engine operating regimes. A comparison between the determined and calculated values of the combustion model's parameters, as presented in Table 4 implies good accuracy of the proposed sub-model. Some differences between the predicted and measured results of the values can be seen but they are rather small. A sub-model was developed based on the experimental results obtained on one specific test engine, thus they may be used with reasonable confidence for the determination of combustion model's parameters for similar engines (M-combustion system and similar operating regimes). For wider use of the sub-model several different measurements should be performed on different engine speed and different throttle positions. The proposed sub-model represents a novelty in this field of combustion model parameters' determination it also presents a step further in the ability of numerical simulation to reduce dependency on experimental measurements.
- The development of similar sub-models for the determination of model parameters can be performed for different engine tips. They could reduce the time needed for performing the numerical simulations of biofuels' influences on engine and emission characteristics.

Acknowledgements

This work was supported by the Slovenian Research Agency (ARRS). We also wish to thank AVL LIST GmbH for their support by providing the AVL-AST software program used during the research.

References

[1] Markovič-Hribernik T, Murks Bašič A. Slovenia's climate policy efforts: CO_2 tax and implementation of EU ETS. Clim Policy 2007;7(2):139–55.
[2] Ajanovic A. Biofuels versus food production: does biofuels production increase food price? Energy 2011;36.
[3] Timilisina GR, Shrestha A. How much hope should we have for biofuels? Energy 2011;36.
[4] Yusuf NNAN, Kamarudin SK, Yaakub Z. Overview on the current trends in biodiesel production. Energy Convers Manage 2011;52:2741–51.
[5] Maghbuly A, Yang W, An H, Li J, Chou SK, Chua KJ. An advance combustion model coupled with detailed chemical reaction mechanism for DI diesel engine simulation. Appl Energy 2013;111:758–70.
[6] Park SH, Cha J, Lee CS. Impact of biodiesel in bioethanol blended diesel on the engine performance and emissions characteristics in compression ignition engine. Appl Energy 2012;99:334–43.
[7] Thumheer T, Edenhauser D, Soltic P, Schreiber D, Kirchen P, Sankowski A. Experimental investigation on different injection strategies in a heavy-duty diesel engine: emissions and loss analysis. Energy Convers Manage 2011;52:457–67.
[8] Roy MM, Wang W, Bujold J. Biodiesel production and comparison of emissions of a DI diesel engine fueled by biodiesel–diesel and canola oil–diesel blends at high idling operations. Appl Energy 2013;106:198–208.
[9] Silitonga AS, Masjuki HH, Mahlia TMI, Ong Hwai Chyuan, Chong WT. Experimental study on performance and exhaust emissions of a diesel engine fuelled with *Ceiba pentandra* biodiesel blends. Energy Convers Manage 2013;76:828–36.
[10] Qi DH, Lee CF, Jia CC, Wang PP, Wu ST. Experimental investigation of combustion and emission characteristics of rapeseed oil–diesel blends in a two cylinder agricultural diesel engine. Energy Convers Manage 2014;77:227–32.
[11] Kegl B. Influence of biodiesel on engine combustion and emission characteristics. Appl Energy 2011;88:1803–12.
[12] Hribernik A, Kegl B. Influence of biodiesel fuel on the combustion and emission formation in a direct injection (DI) diesel engine. Energy Fuels 2007;21:1760–7.
[13] Kegl B. NO_x and particulate matter (PM) emissions reduction potential by biodiesel usage. Energy Fuels 2007;21:3310–6.
[14] Yamane K, Ueta A, Shimamoto Y. Influence of physical and chemical properties of biodiesel fuel on injection, combustion and exhaust emission characteristics in a DI–CI engine. In: The fifth international symposium on diagnostics and modeling of combustion in internal combustion engines (COMODIA), vol. 402; 2001. p. 409.
[15] Holwan DB, Joshi SV. Performance, emission and combustion characteristic of a multicylinder DI diesel engine running on diesel–ethanol–biodiesel blends of high ethanol content. Appl Energy 2011;88:5042–55.
[16] Ushakov S, Valland H, Æsøy V. Combustion and emissions characteristics of fish oil fuel in a heavy-duty diesel engine. Energy Convers Manage 2013;65:228–38.
[17] Labeckas G, Slavinskas S. Performance and emission characteristics of a direct injection diesel engine operating on KDV synthetic diesel fuel. Energy Convers Manage 2013;66:173–88.
[18] Makareviciene V, Sendzikiene E, Pukalskas S, Rimkus A, Vegneris R. Performance and emission characteristics of biogas used in diesel engine operation. Energy Convers Manage 2013;75:224–33.
[19] Palash SM, Kalam MA, Masjuki HH, Arbab MI, Masum BM, Sanjid A. Impacts of NO_x reducing antioxidant additive on performance and emissions of a multi-cylinder diesel engine fueled with Jatropha biodiesel blends. Energy Convers Manage 2014;77:577–85.
[20] Macor A, Avella F, Faedo D. Effect of 30% v/v biodiesel/diesel fuel blends on regulated and unregulated pollutant emissions from diesel engines. Appl Energy 2011;88:4989–5001.
[21] Prah I, Katrašnik T. Application of optimization techniques to determine parameters of the Vibe combustion model. J Mech Eng 2009;55:715–26.
[22] Kegl B. Effects of biodiesel on emissions of a bus diesel engine. Bioresour Technol 2008;99:863–73.
[23] Torres Jiménez E, Kegl M, Dorado R, Kegl B. Numerical injection characteristics analysis of various renewable fuel blends. Fuel 2012;97:832–42.
[24] Dobovišek Ž, Černej A, Hribernik A. Predictive zero-dimensional single-zone diesel combustion simulation models. J Mech Eng 1993;39:137–60.
[25] Chmela F, Orthaber G. Rate of heat release prediction for direct injection diesel engines based on purely mixing controlled combustion. SAE technical paper 1999-01-0186.
[26] Pattas K, Häfner G. Stickoxidbildung bei der ottomotorischen Verbrennung. MTZ 1973;12:397–404.
[27] Onorati A, Ferrari G, D'Errico G. 1D unsteady flows with chemical reactions in the exhaust duct-system of S.I. engines: predictions and experiments. SAE technical paper 2001-01-0939.
[28] AVL List GmbH, AVL BOOST theory, AVL List GmbH, Graz, v2012 ed.; 2010.
[29] Lešnik L, Vajda B, Žunič Z, Škerget L, Kegl B. The influence of biodiesel fuel on injection characteristics, diesel engine performance, and emission formation. Appl Energy 2013;111:558–70.
[30] Kegl B. An improved mathematical model of conventional FIE processes. SAE technical paper 1995-950079.